



## Influence of main channel structure on H<sub>2</sub>O<sub>2</sub> access to the heme cavity of catalase KatE of *Escherichia coli*

Vikash Jha<sup>a</sup>, Prashen Chelikani<sup>a</sup>, Xavi Carpena<sup>b</sup>, Ignacio Fita<sup>b</sup>, Peter C. Loewen<sup>a,\*</sup>

<sup>a</sup> Department of Microbiology, University of Manitoba, Winnipeg, MB, Canada R3T 2N2

<sup>b</sup> IBMB-CSIC/IRB Barcelona, Baldiri i Reixac 10-12, 08028 Barcelona, Spain

### ARTICLE INFO

#### Article history:

Received 24 May 2012

and in revised form 28 June 2012

Available online 20 July 2012

#### Keywords:

Catalase

KatE

Channel architecture

Side chain modification

### ABSTRACT

The main channel for H<sub>2</sub>O<sub>2</sub> access to the heme cavity in large subunit catalases is twice as long as in small subunit catalases and is divided into two distinct parts. Like small subunit catalases, the 15 Å of the channel adjacent to the heme has a predominantly hydrophobic surface with only weak water occupancy, but the next 15 Å extending to the protein surface is hydrophilic and contains a complex water matrix in multiple passages. At the approximate junction of these two sections are a conserved serine and glutamate that are hydrogen bonded and associated with H<sub>2</sub>O<sub>2</sub> in inactive variants. Mutation of these residues changed the dimensions of the channel, both enlarging and constricting it, and also changed the solvent occupancy in the hydrophobic, inner section of the main channel. Despite these structural changes and the prominent location of the residues in the channel, the variants exhibited less than a 2-fold change in the *k*<sub>cat</sub> and apparent *K*<sub>M</sub> kinetic constants. These results reflect the importance of the complex multi-passage structure of the main channel. Surprisingly, mutation of either the serine or glutamate to an aliphatic side chain interfered with heme oxidation to heme d.

© 2012 Elsevier Inc. All rights reserved.

### Introduction

Hydrogen peroxide (H<sub>2</sub>O<sub>2</sub>)<sup>1</sup> is a common byproduct of cellular metabolism, but is inherently dangerous to the cell because of its strong oxidative properties. Several enzymatic systems have evolved to remove H<sub>2</sub>O<sub>2</sub> and reduce the potential for cellular damage of which the most efficient are the catalases with turnover rates in the range of 10<sup>4</sup>–10<sup>6</sup> per second. There are three distinct families of catalases including the heme-containing monofunctional catalases, the heme-containing catalase-peroxidases and the non-heme but manganese-containing catalases [1]. All catalyze the dismutation of H<sub>2</sub>O<sub>2</sub> (2H<sub>2</sub>O<sub>2</sub> → 2H<sub>2</sub>O + O<sub>2</sub>), albeit by different mechanisms.

The monofunctional catalases can be grouped into three phylogenetically related clades, two with small ~60,000 Da subunits (clades 1 and 3) and one with large 80,000 Da subunits (clade 2) found in both bacteria and fungi [2]. A large subunit catalase was the presumed progenitor [2] selected for its enhanced resistance to heat denaturation and protease cleavage [3,4]. Small subunit enzymes subsequently arose by the removal of ~50 residues from the N-terminus and ~150 residues, folded as a flavodoxin-like domain, from the C-terminus. Crystal structures have been reported for at least one representative

of all three clades, revealing a remarkably conserved protein core and homotetrameric structure. Among the clade 2 enzymes, the structures of *Escherichia coli* KatE (also hydroperoxidase or HPII) and 35 of its variants have been reported [5,6] or deposited with the Protein Data Base along with those of *Neurospora crassa* CAT-1 [7] and CAT-3 [8], providing many insights into the catalytic process.

The main channels leading to the heme cavity are about 15 Å longer in large subunit compared to small subunit catalases with a complicated multi-passage architecture (Fig. 1). The channel structure arises from a helical segment containing E530 (KatE numbering is used throughout) folded across what would be the channel entrance in most small subunit enzymes, very likely forced into this position by the longer C-terminus. Also inserted into the side of the channel of large catalases is a four residue sequence containing S234 with its –OH hydrogen bonded (2.7 Å) to the carboxylate of E530. This places the S234–E530 pair at the junction between the relatively hydrophobic lower portion of the channel containing an interrupted chain of low occupancy waters (Fig. 1) and the more hydrophilic extension containing a complex matrix of waters extending to the surface of the protein. In addition, the S234–E530 pair creates a slight constriction in the channel although two waters are hydrogen bonded across the narrowest region (Fig. 1). Otherwise the longer channel is unobstructed, similar to small subunit enzymes, and the added length is not a factor in the slow turnover rates of large subunit enzymes compared to small catalases [9,10].

\* Corresponding author. Fax: +1 204 474 7603.

E-mail address: [peter\\_loewen@umanitoba.ca](mailto:peter_loewen@umanitoba.ca) (P.C. Loewen).

<sup>1</sup> Abbreviation used: H<sub>2</sub>O<sub>2</sub>, hydrogen peroxide.

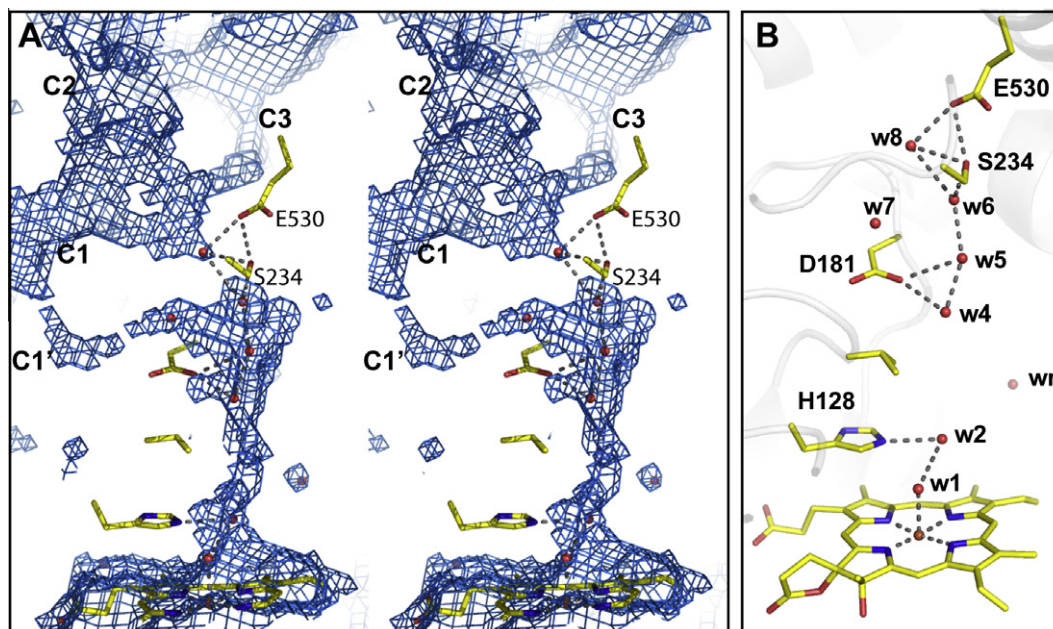


**Fig. 1.** (A) Stereo diagram showing the main channel architecture in KatE. The complexity of the channel above S234 and E530 is evident in the trifurcation into channels C1–C1', C2 and C3. The channel cavities were calculated using VOIDOO. (B) Key residues and waters in the lower part of the channel. Possible hydrogen bond interactions are shown by dashed lines. The numbering of the waters is correlated with Table 3. Water 'wr' or reference water is a high occupancy water in the heme cavity.

A computational analysis of  $\text{H}_2\text{O}_2$  binding to *N. crassa* CAT-1 identified a  $\text{H}_2\text{O}_2$  binding site in the main channel at the equivalent residues to S234 and E530, and it was suggested that they may be actively controlling or gating  $\text{H}_2\text{O}_2$  access to the heme cavity [11]. Experimental validation of the predicted binding site existed in the previously published structure of the  $\text{H}_2\text{O}_2$ -soaked H128N variant of KatE where one  $\text{H}_2\text{O}_2$  is hydrogen bonded to S234 and E530 in addition to the two in the heme cavity [12]. Furthermore, Glu530 is 100% conserved in large subunit catalases while S234 is ~50% conserved with Thr replacing it in the other ~50%. In this report, the roles of S234 and E530 are investigated in an analysis of the kinetic and structural properties of a series of variants mutated in the two residues.

## Materials and methods

### Variant protein construction, purification and characterization

Standard chemicals and biochemicals were obtained from Sigma. The oligonucleotides CAAGGGCAAGCTGCCACGATA (S234A), CAAGGGCAAGATGCCACGATA (S234D), CAAGGGCAAAATGCCACGATA (S234N), CAAGGGCAAATGCCACGATA (S234I), CAAGGCAATGGGCCACGATA (S234W), TTCAGTTTTGCTTTAAGCAAA (E530A), TTCAGTTTTGATTTAAGCAAA (E530D), TTCAGTTTTATTTAAGCAAA (E530I), and TTCAGTTTTAGTTAAGCAAA (E530Q), were purchased from Invitrogen and used to mutate the *Hind*III–*Eco*RI (base pairs 1246–1856) or *Eco*RI–*Clal* fragment (base pairs 1856–3466) of pAMkatE72 [13] following the Kunkel procedure [14] as previously described [15]. The mutated sequences were confirmed [16] and used to generate the plasmids pS234A, pS234D, pS234N, pS234I, pS234W, pE530A, pE530D, pE530I and pE530Q by reincorporating the fragment into the full length *katE* gene. The native and variant proteins were expressed and purified as described [15]. Catalase activity was determined by the method of Rørth and Jensen [17] in a 1.8 mL reaction volume using a Gilson oxygraph equipped with a Clark electrode. One unit of catalase is defined as the amount that decomposes 1  $\mu\text{mol}$  of  $\text{H}_2\text{O}_2$  in 1 min in a 60 mM  $\text{H}_2\text{O}_2$  solution at pH 7.0 and 37 °C. The initial rates of

oxygen evolution were used to determine the turnover rates ( $k_{\text{cat}}$ ) and apparent  $K_{\text{M}}$  values (Table 1). Protein was estimated according to the methods outlined by Layne [18]. All spectra were obtained using a Milton Roy MR3000 spectrophotometer.

### Crystallization and structure determination

Crystals of the HPII variants were obtained at 22 °C using the hanging drop vapor diffusion method over a reservoir solution containing 15–17% PEG 3350 (Carbowax), 1.6–1.7 M LiCl and 0.1 M Tris pH 9.0 [5,6]. The crystals were monoclinic, space group  $P2_1$  with one tetrameric molecule in the crystal asymmetric unit. Data sets were collected using synchrotron beam line CMCF 08ID-1 at the Canadian Light Source in Saskatoon, Canada from crystals flash cooled in the reservoir buffer. Diffraction data were processed and scaled using programs MOSFLM and SCALA [19], respectively (Table 2). Structure refinement starting with native KatE structure (1GGE) was completed using program REFMAC [20] and manual modeling with the molecular graphics program COOT [21]. The Ramachandran distribution of residues for all structures was

**Table 1**  
Kinetic comparison of the S234 and E530 variants.

Variant	$k_{\text{cat}}$ ( $\text{s}^{-1}$ )	$K_{\text{M}}(\text{app})^a$ (mM)	$k_{\text{cat}}/K_{\text{M}}(\text{app})$ ( $\text{s}^{-1} \text{M}^{-1}$ )
WT	100,780	220	$4.6 \times 10^5$
S234A	88,800	460	$1.9 \times 10^5$
S234I	162,700	680	$2.4 \times 10^5$
S234D	100,500	370	$2.7 \times 10^5$
S234N	84,900	265	$3.2 \times 10^5$
E530A	182,000	675	$2.7 \times 10^5$
E530I	96,500	575	$1.7 \times 10^5$
E530D	71,200	165	$4.3 \times 10^5$
E530Q	75,000	560	$1.3 \times 10^5$
E530A/S234A	189,800	320	$6.7 \times 10^5$

<sup>a</sup>  $K_{\text{M}}(\text{app})$ – $K_{\text{M}}(\text{apparent})$  in the context of catalases is the  $\text{H}_2\text{O}_2$  concentration at  $1/2 V_{\text{max}}$  and is used because the catalytic reaction does not strictly saturate with substrate and therefore does not precisely follow Michaelis–Menten kinetics [7]. Large subunit catalases are very resistant to inhibition or damage at high  $[\text{H}_2\text{O}_2]$  allowing up to 5 M  $\text{H}_2\text{O}_2$  to be used in assays.

**Table 2**  
Data collection and refinement statistics.

A – data collection statistics								
Variant	E530A	E530D	E530I	E530Q	S234A	S234D	S234I	S234N
PDB	4ENP	4ENQ	4ENR	4ENS	4ENT	4ENU	4ENV	4ENW
Unit cell parameters								
a (Å)	93.33	93.38	93.58	93.45	93.46	93.56	93.23	93.39
b (Å)	133.11	133.09	132.78	133.40	133.05	132.61	133.13	132.57
c (Å)	122.74	122.34	122.81	123.24	122.19	122.81	122.71	122.57
Resolution <sup>a</sup>	35.2–1.5 (1.58–1.50)	41.4–1.9 (2.00–1.90)	34.2–1.6 (1.69–1.60)	32.2–1.6 (1.69–1.60)	33.3–1.7 (1.79–1.70)	33.2–1.7 (1.79–1.70)	34.2–1.7 (1.79–1.70)	35.1–1.90 (2.00–1.90)
Unique reflections	449780 (65633)	204992 (29254)	357773 (49514)	344208 (42156)	302611 (41894)	284036 (36029)	246545 (29305)	206796 (27496)
Completeness%	99.9 (100.0)	92.4 (90.5)	96.3 (91.5)	92.1 (77.6)	98.2 (93.5)	92.0 (80.3)	79.9 (65.3)	93.6 (85.5)
R <sub>merge</sub>	0.079 (0.288)	0.065 (0.245)	0.094 (0.453)	0.099 (0.351)	0.110 (0.554)	0.059 (0.201)	0.062 (0.188)	0.086 (0.238)
<I/σI>	9.4 (3.9)	9.0 (3.0)	7.9 (2.6)	7.4 (2.5)	7.9 (2.5)	13.9 (5.0)	7.5 (2.9)	8.7 (4.9)
Multiplicity	3.8 (3.6)	2.0 (2.1)	3.5 (3.4)	3.2 (2.7)	3.3 (3.2)	3.5 (3.2)	2.1 (1.8)	3.2 (2.7)
B – Model refinement statistics								
Reflections	427158	194502	339252	326323	287023	269541	233265	196178
R <sub>cryst</sub> (%)	13.8	15.8	15.8	15.1	15.8	13.4	16.7	17.5
R <sub>free</sub> (%)	16.2	20.7	19.3	18.4	19.7	17.0	20.7	22.1
Non-H atoms	26707	26325	26152	26323	26318	26278	26351	25927
No. waters	3344	3167	2948	2948	2981	3053	3010	2752
Average B-factor Å <sup>2</sup>								
Protein	16.3	15.5	14.6	15.2	14.0	14.2	15.0	14.7
Heme	9.0	9.5	7.2	7.5	6.1	8.3	8.5	8.9
Waters	26.6	22.0	24.4	25.1	24.5	23.8	23.3	22.7
Other								
Coor. err. Å <sup>b</sup>	0.036	0.091	0.057	0.051	0.066	0.052	0.068	0.092
rms dev bonds Å	0.027	0.020	0.025	0.025	0.022	0.024	0.021	0.019
rms dev. angles °	2.65	2.05	2.49	2.57	2.45	2.33	2.38	2.07

<sup>a</sup> Values in parentheses correspond to the highest resolution shell.

<sup>b</sup> Based on maximum likelihood.

~96%, 3.5% and 0.5%, respectively, in favored, allowed and outlier regions. Figures were generated using PYMOL (The PYMOL Molecular Graphics System, Schrödinger, LLC).

The coordinates for the structures included in this manuscript have been submitted with PDB accession codes 4ENP (E530A), 4ENQ (E530D), 4ENR (E530I), 4ENS (E530Q), 4ENT (S234A), 4ENU (S234D), 4ENV (S234I) and 4ENW (S234N).

## Results and discussion

### Kinetic characterization of the S234 and E530 variants

The residues equivalent to S234 and E530 in *N. crassa* CAT-1 (S198 and E489) were identified as components of a putative gate controlling access of H<sub>2</sub>O<sub>2</sub> to the heme cavity [11]. They are also notable because of their conservation, their location at the junction between the hydrophobic inner and hydrophilic outer sections of the main channel with unobstructed paths between their side chains and the heme iron 17–20 Å distant, and their association with H<sub>2</sub>O<sub>2</sub> in an inactive KatE variant [12]. To investigate the influence of the side chains on the catalytic reaction, mutations to acidic, uncharged polar, and aliphatic side chains were introduced. Specifically, plasmids harboring mutated *katE* genes encoding S234A, S234D, S234N, S234I, S234W, E530A, E530Q, E530D and E530I were constructed. All variants except S234W accumulated normal amounts of protein confirming that protein folding was not affected by any of the changes except to the indole ring.

Determination of the kinetic parameters of the variants revealed relatively minor changes compared to the wild type enzyme (Table 1). The turnover rates are unchanged or slightly reduced with the exceptions of S234I, E530A and the double mutant S234A/E530A for which the  $k_{cat}$  values are increased by 60–80%. All but one of the variants had increased apparent  $K_M$ 's ( $K_M\{app\}$ )

for H<sub>2</sub>O<sub>2</sub> and the apparent catalytic efficiency expressed as  $k_{cat}/K_M\{app\}$  is reduced by 30–50% in all cases except E530D and the double variant. (Table 1). It is important to note that the  $K_M\{app\}$  in the context of catalases is the observed H<sub>2</sub>O<sub>2</sub> concentration at 1/2  $V_{max}$  and is used because the catalytic reaction does not saturate with substrate and therefore does not precisely follow Michaelis–Menten kinetics [9].

In summary, the catalytic efficiencies of the S234 and E530 variants were remarkably similar across a variety of side chains. This is consistent with previous kinetic and structural work that concluded the extended main channel of large subunit enzymes has no substantive effect on catalytic turnover and only a minor impact on substrate access reflected in the 2-fold higher  $K_M\{app\}$  for H<sub>2</sub>O<sub>2</sub>.

### Structural characterization of the S234 and E530 variants

To provide a better picture of the effect of the mutations on solvent occupancy in the main channel and heme cavity, the structures of the eight variants were determined by X-ray crystallography (Table 2). All refined to between 1.5 and 1.9 Å providing a uniform high resolution picture of the side chains, channel size and solvent complement. The expected modified side chain was evident in each variant and its presence was verified in  $F_o - F_c$  omit maps calculated without the side chain in the model (Supplementary information). The mutations caused no change in the locations or orientations of surrounding residues compared to the wild type enzyme.

Two features, aside from the mutated side chains, differ among the variants. In contrast to the relative invariance of solvent in other channels and cavities among the different variants, the lower part of the main channel is the site of considerable variation (Table 3). At one extreme is E530I in which the lower main channel is essentially devoid of solvent (only w2 is present in all subunits)

(Table 3). Two other aliphatic replacement variants E530A and S234I, and the uncharged, polar variant S234N, also have reduced solvent occupancy compared to the native enzyme although E530A has a full complement of w5\*, w6 and w7 high in the channel. By contrast, the aliphatic replacement variant, S234A, resembles E530Q, E530D and S234D with a solvent complement similar to the native enzyme, albeit with some small shifts in solvent locations. All of the variable waters, including w1 and w3–7, have elevated B values (>20 Å<sup>2</sup>) suggesting low occupancy. Significantly, w8, which is hydrogen bonded to S234 in the native

enzyme, essentially at the site of H<sub>2</sub>O<sub>2</sub> binding in the inactive variant, is conserved in all subunits of all variants.

The second difference among the variants lies in their channel architectures (Fig. 2). Two variants, S234A and E530I, present a slightly more open or continuous channel adjacent to S234 whereas S234I, S234D and S234N present a 7–8 Å gap that might be inferred to present an obstruction to movement down the channel. The corresponding channel segments in the remaining three E530 variants were largely unchanged compared to the native enzyme. There is surprisingly little correlation between channel

**Table 3**

B values (Å<sup>2</sup>) of waters in the main channel and heme cavity of KatE, its variants and CAT-1.

**Table 3**

B values (Å<sup>2</sup>) of waters in the main channel and heme cavity of KatE, its variants and CAT-1.

KatE (heme d), 1GGE				CAT-1 (0.4 heme d, 0.6 heme b), 1SY7					
	A	B	C	D		A	B	C	D
w1	30.9	32.6	29.9	29.1	w1	–	–	–	–
w2	12.9	16.5	15.2	13.8	w2	19.0	–	21.8	–
w3	– <sup>a</sup>	–	39.2	28.9	w3	22.4	–	24.4	–
w4	28.1	33.2	34.6	31.8	w4	58.9	–	45.7	–
w5	46.9	38.9	43.3	38.5	w5	32.4	–	37.0	–
w6	15.2	17.2	25.4	14.1	w6	18.0	–	20.5	–
w7	32.4	34.7	35.8*	32.1	w7	–	–	–	–
w8	7.7	10.9	18.6	6.6	w8	18.9 <sup>†</sup>	–	16.1 <sup>†</sup>	–
wr <sup>b</sup>	7.1	9.0	8.5	7.6	wr	13.5	–	14.5	–
S234I (0.6 heme d, 0.4 heme b), 4ENV				S234A (0.7 heme d, 0.3 heme b), 4ENT					
w1	23.8	26.0	27.8	–	w1	35.6 <sup>†</sup>	37.3	42.5 <sup>†</sup>	–
w2	13.8	17.9	15.2	13.3	w2	19.1	26.5	25.3	19.4
w3	–	–	–	–	w3	–	–	–	–
w4	–	33.9	33.7	41.4	w4	44.9	36.5	36.2	39.9
w5	–	–	–	–	w5	32.3	27.6 <sup>†</sup>	27.3 <sup>†</sup>	26.5 <sup>†</sup>
w6	–	–	–	–	w6	24.8	32.9	27.2	23.6
w7	–	–	–	–	w7	24.5	27.3	24.8	22.4
w8	21.6	22.1	24.9	23.7	w8	17.0	17.2	20.0	15.0
wr	9.8	10.2	10.1	7.6	wr	9.5	8.4	10.1	8.2
S234D (heme d), 4ENU				S234N (heme d), 4ENW					
w1	42.2	34.0	37.9	35.9 <sup>†</sup>	w1	41.1	31.3	41.3 <sup>†</sup>	39.7 <sup>†</sup>
w2	17.4	22.9	19.3	19.2	w2	16.7	18.0	15.0	16.3
w3	–	–	39.1	–	w3	–	–	–	32.8 <sup>†</sup>
w4	43.4	32.7	34.2	27.1	w4	–	37.8	33.7	–
w5	25.4	21.4	24.5	21.2	w5	–	30.8	28.7	23.6
w6	31.6 <sup>†</sup>	27.9 <sup>†</sup>	27.9 <sup>†</sup>	25.7 <sup>†</sup>	w6	–	–	–	–
w7	24.8	26.7	–	22.5	w7	25.3	26.8	–	21.4
w8	20.0	17.6	20.9	18.0	w8	22.4	20.6	19.9	12.5
wIII	7.4	10.3	10.0	8.9	wIII	9.1	10.8	11.0	10.9
E530I (heme b), 4ENR				E530A (heme b), 4ENP					
w1	–	–	–	–	w1	–	–	–	–
w2	24.6	30.7	24.9	23.0	w2	16.5	19.7	17.6	16.2
w3	–	–	–	–	w3	–	–	–	–
w4	–	–	–	–	w4	–	–	–	–
w5	–	–	–	38.1 <sup>†</sup>	w5	26.0 <sup>†</sup>	29.5 <sup>†</sup>	25.5 <sup>†</sup>	27.0 <sup>†</sup>
w6	–	–	–	31.7 <sup>†</sup>	w6	23.4	25.8	24.6	23.8
w7	25.3	25.2	–	32.3	w7	21.4	24.2	22.8	21.8
w8	16.4	16.9	18.9	15.6	w8	21.4	22.6	21.8	17.9
wr	7.9	9.2	10.7	8.5	wr	9.9	11.4	11.6	10.4
E530Q (0.7 heme d, 0.3 heme b), 4ENS				E530D (heme d), 4ENQ					
w1	25.6	22.7	29.6	27.4	w1	20.9	24.5	28.1	–
w2	15.6	20.7	16.5	16.7	w2	15.5	15.0	15.3	18.2
w3	–	–	–	–	w3	–	–	–	–
w4	46.3	42.6	33.1	41.4	w4	37.3	–	–	–
w5	–	45.6	40.1 <sup>†</sup>	47.0	w5	24.3 <sup>†</sup>	30.1 <sup>†</sup>	21.7 <sup>†</sup>	31.0 <sup>†</sup>
w6	14.7	17.8	18.8	14.9	w6	11.1	10.0	10.9	13.4
w7	30.0	36.0	–	38.9	w7	22.3	23.9	18.9	18.4
w8	13.2	16.6	14.8	15.3	w8	18.3	10.5	9.4	6.3
wr	9.2	11.7	12.5	10.8	wr	7.0	7.0	6.1	6.8

<sup>†</sup>Denotes waters shifted slightly (1–1.5 Å) from the position in 1GGE.

<sup>a</sup>Locations where waters are missing are colored grey for visual impact.

<sup>b</sup>wr or Reference water is a high occupancy water in the heme cavity.

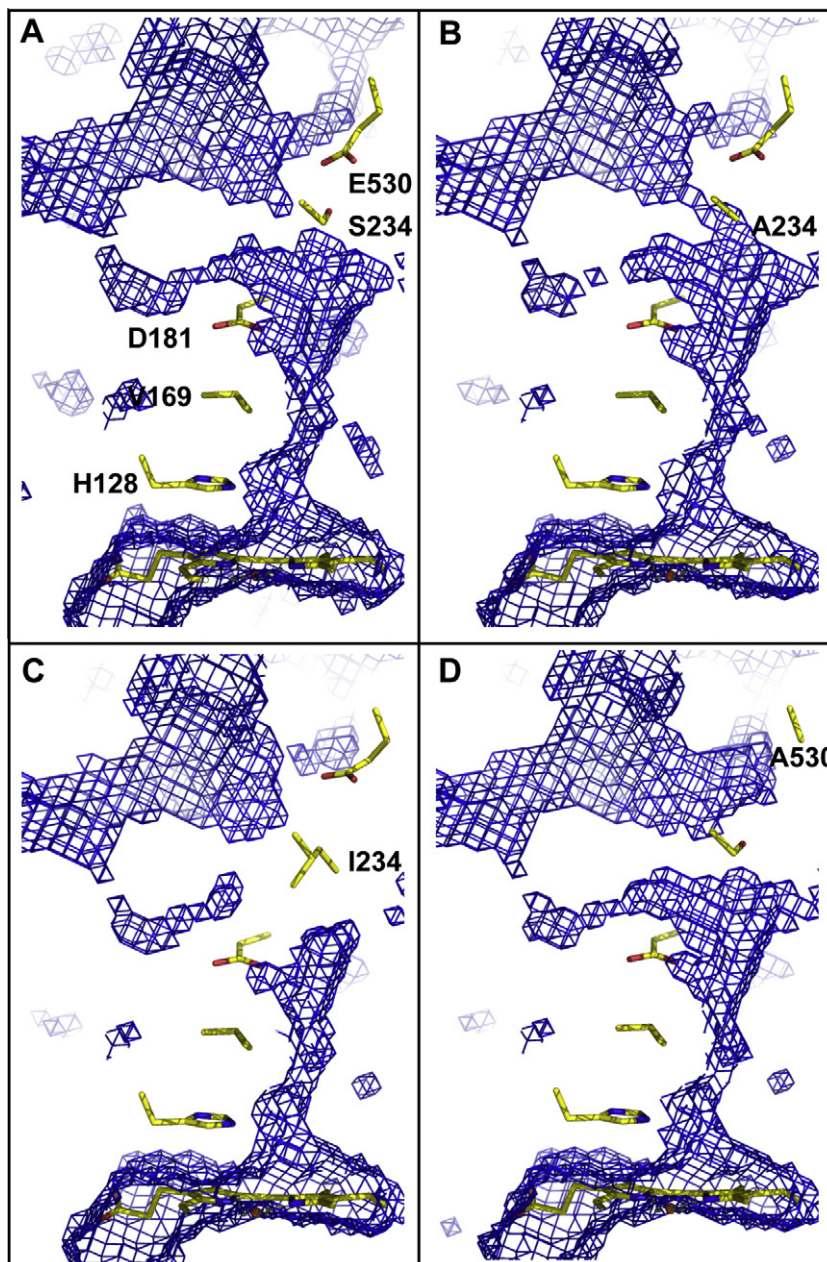


**Fig. 2.** Main channel cavities in native KatE and selected variants. Only the channel in subunit A is shown but channels in the other subunits were similar in a given variant. The channels are shown for (A) native; (B) S234A; (C) S234I; and (D) E530A. The channels in S234N and S234D were similar to S234I (panel C), in E530I, similar to S234A (panel B), and E530Q and E530D, similar to native (panel A). Cavities were calculated using VOIDOO.

dimensions and water occupancy in the hydrophobic section. For example, S234A and E530I present less obstructed channels, but the former has a nearly complete water matrix in the lower channel while the latter is essentially devoid of solvent in that region. In addition, S234I with the most occluded channel exhibits one of the highest turnover rates similar to that of E530A in which the channel dimensions are similar to native.

The importance of  $\text{H}_2\text{O}_2$  retention in the heme cavity, presumably to maintain a critical substrate concentration for reactivity, was demonstrated by the reduction in catalytic efficiency (from  $4.6$  to  $0.1 \times 10^6 \text{ s}^{-1} \text{ M}^{-1}$ ) when the opening into the lateral channel was enlarged [22]. By comparison, however, the main channel is very open and neither constriction nor enlargement at S234 has a significant impact on reaction rate. Two other factors may be at

play. The first is an inherent attraction of  $\text{H}_2\text{O}_2$  to the heme cavity, evident in two  $\text{H}_2\text{O}_2$  being bound in the heme cavity of the inactive variant. The electrical potential field between the conserved aspartate (D181 in Fig. 1) and heme iron which aligns the electrical dipoles of  $\text{H}_2\text{O}$  and  $\text{H}_2\text{O}_2$  thereby optimizing the molecular orientation for binding [15] may be an important component of this apparent attraction. Secondly, the lower part of the channel between S234 and the heme is hydrophobic providing no binding sites for  $\text{H}_2\text{O}_2$  and supporting only a low occupancy matrix of solvent.

It is tempting to draw an analogy between the passage of water through aquaporins [23–25] and the passage of  $\text{H}_2\text{O}_2$  and  $\text{H}_2\text{O}$  through the main channel of large subunit catalases. Like one side of an aquaporin, the outer hydrophilic portion of the

KatE channel presents a continuous chain or matrix of waters leading to a narrow constriction at the serine–glutamate pair (two asparagines in aquaporins). On the other side of the constriction, however, the two systems are very different with aquaporins presenting a near mirror image chain of linked waters, whereas KatE presents a low occupancy, discontinuous chain of solvent making few contacts with the hydrophobic surface of the channel. Furthermore, whereas the double asparagine motif at the constriction in aquaporins is critical for the preclusion of proton transport, the serine–glutamate motif appears to have little function.

In summary, there is no consistent correlation among the mutations, the kinetic changes, the solvent occupancies or the changes in architecture in the variant channels. (a) Aliphatic side chains reduce water occupancy in three cases but not in the fourth. (b) The uncharged but polar N234, but not Q530, reduces solvent occupancy. (c) Reduced solvent occupancy is paired with high turnover rates in S234I and E530A. (d) The water matrix in the vicinity of residues 234 and 530 is largely unchanged across the range of variants. (e) The turnover rates are relatively unchanged in all variants except S234I and E530A. (f) The high turnover rate of S234I occurs despite occlusion of the channel. The only consistency among the variants is an increase in  $K_M$  for  $H_2O_2$  in six of the S234 and E530 variants; only S234N and E530D were unchanged compared to native. Thus, the hydrogen bonded residues S234 and E530 situated at the junction of the inner hydrophobic and outer hydrophilic sections may be the last point of association for  $H_2O_2$  with the protein before reaching the heme, but have only a minor role in facilitating  $H_2O_2$  passage to the heme cavity.

#### *Influence of S234 and E530 on heme oxidation to heme d*

The absorbance spectra of the variants and native enzyme differ only in the region of the charge transfer bands suggesting the presence of differing proportions of heme d (590 nm) and heme b (630 nm) (data not shown). This was confirmed by HPLC and in the crystal structures that revealed the aliphatic variants, S234A, S234I, E530I and E530A to contain more heme b (100% in the case of E530A and E530I) than heme d. Previously, heme b in native KatE, prepared under anaerobic conditions, had been converted to heme d by ascorbate treatment [26], but the heme b in both E530A and E530I proved to be resistant to such treatment (data not shown). Thus, despite only a minor effect on the catalytic reaction, S234 and E530 appear to have a role modulating the post-translational oxidation of the heme b to heme d. Small variations in the ratio of heme b and heme d in variants of KatE have been noted previously [22], and were associated with residue changes in close proximity to the heme as well as variations in aeration or growth conditions. The remoteness of E530 from the heme combined with the absence of any conversion to heme d preclude these previous explanations, and  $H_2O_2$  accessibility does not seem to be impaired in these variants. In the absence of such clear explanations, we are left for the moment with a more tenuous suggestion of an inductive effect of the polar side chain at residue 530.

## Acknowledgments

This work was supported by a Discovery Grant 9600 from the Natural Sciences and Engineering Research Council of Canada and by the Canada Research Chair Program (to P.C.L.). Research described in this paper was performed at the Canadian Light Source, which is supported by the Natural Sciences and Engineering Research Council of Canada, the National Research Council Canada, the Canadian Institutes of Health Research, the Province of Saskatchewan, Western Economic Diversification Canada, and the University of Saskatchewan.

## Appendix A. Supplementary data

Supplementary data associated with this article can be found, in the online version, at <http://dx.doi.org/10.1016/j.abb.2012.06.010>.

## References

- [1] P. Nicholls, I. Fita, P.C. Loewen, *Adv. Inorg. Chem.* 51 (2001) 51–106.
- [2] M.G. Klotz, P.C. Loewen, *Mol. Biol. Evol.* 20 (2003) 1098–1112.
- [3] J. Switala, J. O'Neil, P.C. Loewen, *Biochemistry* 38 (1999) 3895–3901.
- [4] P. Chelikani, L.J. Donald, H.W. Duckworth, P.C. Loewen, *Biochemistry* 42 (2003) 5729–5735.
- [5] J. Bravo, N. Verdaguier, J. Tormo, C. Betzel, J. Switala, P.C. Loewen, I. Fita, *Structure* 3 (1995) 491–502.
- [6] J. Bravo, M.J. Maté, T. Schneider, J. Switala, K. Wilson, P.C. Loewen, I. Fita, *Proteins* 34 (1999) 155–166.
- [7] A. Díaz, E. Horjales, E. Rudiño-Piñera, R. Arreola, W. Hansberg, *J. Mol. Biol.* 342 (2004) 971–985.
- [8] A. Díaz, V.-J. Valdés, E. Rudiño-Piñera, E. Horjales, W. Hansberg, *J. Mol. Biol.* 386 (2009) 218–232.
- [9] J. Switala, P.C. Loewen, *Arch. Biochem. Biophys.* 401 (2002) 145–154.
- [10] P. Chelikani, X. Carpena, R. Perez-Luque, L.J. Donald, H.W. Duckworth, J. Switala, I. Fita, P.C. Loewen, *Biochemistry* 44 (2005) 5597–5605.
- [11] L. Domínguez, A. Sosa-Peinado, W. Hansberg, *Arch. Biochem. Biophys.* 500 (2010) 82–91.
- [12] W. Melik-Adamyant, J. Bravo, X. Carpena, J. Switala, M.J. Maté, I. Fita, P.C. Loewen, *Proteins* 44 (2001) 270–281.
- [13] I. von Ossowski, M.R. Mulvey, P.A. Leco, A. Borys, P.C. Loewen, *J. Bacteriol.* 173 (2001) 514–520.
- [14] T.A. Kunkel, J.D. Roberts, R.A. Zakour, *Meth. Enzymol.* 154 (1987) 367–382.
- [15] P. Chelikani, X. Carpena, I. Fita, P.C. Loewen, *J. Biol. Chem.* 278 (2003) 31290–31296.
- [16] F.S. Sanger, S. Nicklen, A.R. Coulson, *Proc. Natl. Acad. Sci. USA* 74 (1977) 5463–5467.
- [17] H.M. Rørth, P.K. Jensen, *Biochim. Biophys. Acta* 139 (1967) 171–173.
- [18] E. Layne, *Meth. Enzymol.* 3 (1957) 447–454.
- [19] Collaborative Computational Project, *Acta Crystallogr.* D50 (1994) 760–763.
- [20] G.N. Murshudov, A.A. Vagin, E.J. Dodson, *Acta Crystallogr.* D53 (1997) 240–255.
- [21] P. Emsley, K. Cowtan, *Acta Crystallogr.* D60 (2004) 2126–2132.
- [22] V. Jha, S. Louis, P. Chelikani, X. Carpena, L.J. Donald, I. Fita, P.C. Loewen, *Biochemistry* 50 (2011) 2101–2110.
- [23] D. Fu, A. Libson, L.J.W. Miercke, C. Weitzman, P. Nollert, J. Krucinski, R.M. Stroud, *Science* 290 (2000) 481–486.
- [24] P. Noller, W.E.C. Harries, D. Fu, L.J.W. Miercke, R.M. Stroud, *FEBS Lett.* 504 (2001) 112–117.
- [25] E. Tajkhorshid, P. Noller, M.Ø. Jensen, L.J.W. Miercke, J. O'Connell, R.M. Stroud, K. Schulten, *Science* 296 (2002) 525–530.
- [26] P.C. Loewen, J. Switala, I. von Ossowski, A. Hillar, A. Christie, B. Tattrie, P. Nicholls, *Biochemistry* 32 (1993) 10159–10164.